ChemComm

COMMUNICATION

View Article Online
View Journal | View Issue

Cite this: *Chem. Commun.*, 2018, **54**, 12385

Received 1st August 2018,
Accepted 27th September 2018

DOI: 10.1039/c8cc06261g

rsc.li/chemcomm

Redox-dependent conformational changes of a proximal [4Fe–4S] cluster in Hyb-type [NiFe]-hydrogenase to protect the active site from O_2†

Noor Dina Muhd Noor,‡§[ab] Hiroaki Matsuura,‡[ab] Koji Nishikawa,‡[abc] Hulin Tai,‡[bd] Shun Hirota,[bd] Jaehyun Kim,[a] Jiyoung Kang,¶[a] Masaru Tateno,[a] Ki-Seok Yoon,[ef] Seiji Ogo,[ef] Shintaro Kubota,[ag] Yasuhito Shomura[bh] and Yoshiki Higuchi *[abc]

***Citrobacter* sp. S-77 [NiFe]-hydrogenase harbors a standard [4Fe–4S] cluster proximal to the Ni–Fe active site. The presence of relocatable water molecules and a flexible aspartate enables the [4Fe–4S] to display redox-dependent conformational changes. These structural features are proposed to be the key aspects that protect the active site from O_2 attack.**

Hydrogenases catalyze the reversible oxidation of H_2.[1] [NiFe]-hydrogenases are classified into four groups, which are divided further into subgroups.[2] O_2-sensitive "standard" enzymes (STD-type) in Group 1b lose their catalytic activity at ambient O_2 concentrations and produce two inactive forms, Ni-A and Ni-B.[3,4] Ni-B is a "ready" inactive form, whereas Ni-A (with multiple modifications on cysteine ligands by oxygen species[3,5]) is an "unready" inactive form.[6] O_2-tolerant enzymes are catalytically active in the presence of a small amount of O_2, and mainly form Ni-B upon inactivation.[7] Crystal structures of the hydrogenase unit of membrane-bound O_2-tolerant [NiFe]-hydrogenases (MBH-type) in Group 1d from *Hydrogenovibrio marinus* (HmMBH),[8] *Ralstonia eutropha* (ReMBH),[9] and *Escherichia coli* (EcMBH)[10] are almost identical to those in STD-type, but harbor an unprecedented [4Fe–3S]–6Cys ($[4Fe–3S]_P$) cluster proximal to the Ni–Fe active site. $[4Fe–3S]_P$ in the $K_3[Fe(CN)_6]$-oxidized (FOXI) state was deformed from the original structure found in the H_2-reduced (HRED) enzyme, and its redox-dependent conformational changes explain their O_2-stability (Fig. S1A–D and F, ESI†). STD-type enzymes do not have this kind of system, and the lost catalytic activity in the oxidized form is recovered only after the removal of O_2 (Fig. S1E, ESI†). In contrast, the enzymes in Group 1e (Isp-type) are quite sensitive to O_2, and the proximal [4Fe–4S] cluster ($[4Fe–4S]_P$) of the enzyme from *Allochromatium vinosum* (AvISP) was reported to be damaged by O_2, resulting in a dead enzyme.[11]

Alternative membrane-bound enzymes in Group 1c (Hyb-type) from *Citrobacter* sp. S-77 are heterotetrameric enzymes.[12] The hydrogenase unit (S77HYB) is composed of a large subunit that harbors the active site and a small subunit with three Fe–S clusters. S77HYB is stable to O_2 exposure[12] and its activity was recovered from a H_2-containing solution with about 1.0% O_2,[13] indicating that it has a novel O_2 protecting ability, though it lacks two supernumerary cysteine residues at the proximal cluster in MBH-type enzymes. In this study, we have determined the crystal structures of S77HYB in the various redox states. The crystal structures, spectroscopic and theoretical results allowed us to identify how $[4Fe–4S]_P$ of S77HYB contributes to protect the active site from O_2 damage.

The X-ray crystal structures of S77HYB in HRED, air-oxidized (AOXI), and FOXI states were analyzed at resolutions of 1.84, 1.57, and 2.05 Å, respectively (Table S1A, ESI†).‖ The overall structures were similar to the enzymes in Group 1, and the architecture of the formation of two heterodimers (Fig. S2A, ESI†) was almost identical to HmMBH. The estimated root-mean-square deviations of Cα between S77HYB and MBH-type enzymes were 0.4–0.7 Å. The Ni–Fe active site in HRED showed the ligand structure which corresponds to the Ni-C or Ni-R state

[a] *Department of Life Science, Graduate School of Life Science, University of Hyogo, 3-2-1 Koto, Kamigori-cho, Ako-gun, Hyogo 678-1297, Japan. E-mail: hig@sci.u-hyogo.ac.jp*
[b] *Core Research for Evolutional Science and Technology (CREST), Japan Science and Technology Agency (JST), 4-1-8 Honcho, Kawaguchi-shi, Saitama 332-0012, Japan*
[c] *RIKEN SPring-8 Center, 1-1-1 Koto, Sayo-gun, Sayo-cho, Hyogo 679-5148, Japan*
[d] *Division of Materials Science, Graduate School of Science and Technology, Nara Institute of Science and Technology, 8916-5 Takayama, Ikoma, Nara 630-0192, Japan*
[e] *Department of Chemistry and Biochemistry, Graduate School of Engineering, Kyushu University, 744 Moto-oka, Nishi-ku, Fukuoka 819-0395, Japan*
[f] *International Institute for Carbon Neutral Energy Research (WPI-I2CNER), Kyushu University, 744 Moto-oka, Nishi-ku, Fukuoka 819-0395, Japan*
[g] *Institute for Research Promotion and Collaboration, University of Hyogo, 123 Minamiekimae-cho, Himeji, Hyogo 670-0962, Japan*
[h] *Institute of Quantum Beam Science, Graduate School of Science and Engineering, Ibaraki University, 4-12-1 Nakanarusawa, Hitachi, Ibaraki 316-8511, Japan*

† Electronic supplementary information (ESI) available. See DOI: 10.1039/c8cc06261g

‡ These authors are contributed equally to this work.

§ Present address: Enzyme & Microbial Technology Research Centre (EMTech), University Putra Malaysia, 43400 UPM Serdang, Selangor, Malaysia.

¶ Present address: Center for Systems and Translational Brain Sciences, Yonsei University, 50 Yonsei-ro Seodaemun-gu, Seoul, 03722, Republic of Korea.

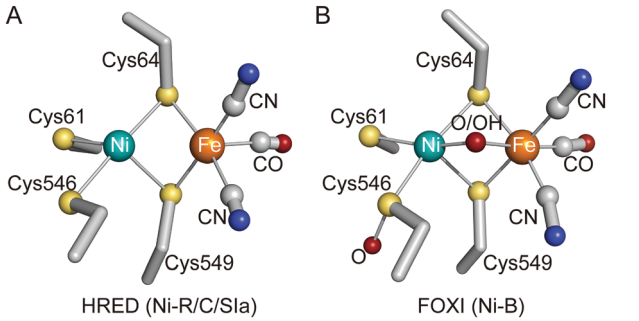

Fig. 1 The Ni–Fe active site of S77HYB in the HRED (A) and FOXI (B) states (atom colors: C, gray; N, blue; O, red; S, yellow; Fe, orange; Ni, green).

without a bridging oxygenic ligand (Fig. 1A and Fig. S2B, ESI†), as indicated by subatomic crystallographic and spectroscopic studies.[14] In contrast, the active sites in FOXI and AOXI showed a typical structure ascribable to the Ni-B state with a bridging ligand between Ni and Fe (Fig. 1B and Fig. S2C, D, ESI†). In solution, Ni-B signals were mainly observed in the EPR spectra of AOXI and FOXI S77HYB (Fig. S3A and B, ESI†), whereas typical Ni-C signals were observed in the HRED spectrum (Fig. S3C, ESI†). HRED and AOXI spectra were reproducible by reduction and oxidation by H_2 and O_2, respectively (Fig. S3C–E, ESI†), indicating the high O_2 stability of S77HYB. The Ni-C and Ni-R signals were observed in the Fourier-transform infrared spectroscopy (FT-IR) spectra of HRED (Fig. S3H, ESI†).

S77HYB contained $[4Fe–4S]_P$ (Fig. 2A). The structures of $[4Fe–4S]_P$ and the neighboring three water molecules (W2–W4) were well conserved in STD- and Isp-type enzymes (Fig. 2D and E). The only differences around the cluster between HRED and FOXI S77HYB were the conformation of Asp81 and W1. In HRED, W1 is within hydrogen bonding distance of the carboxylate group of Asp81 and main-chain N (Thr23, Gly24 and Cys25) (Fig. 2A and Fig. S2E, ESI†). Fe4 in FOXI is shifted by 1.8 Å from the original position in HRED toward Asp81 (Fe4–Oδ1 = 2.0 Å) upon oxidation (Fig. 2B and Fig. S2F, ESI†). W1 in HRED was not assignable in FOXI; instead, S1 was shifted by 1.8 Å toward the W1 site in HRED (S1-N(Thr23) = 3.0 Å) (Fig. 2B). In addition, Fe4 and Fe2 were coordinated by a tentatively assigned oxygen species (O1), with distances of 2.0 and 1.5 Å, respectively. O1 is potentially hydrogen-bonded to W2 assigned in both HRED and FOXI (Fig. 2A and B). $[4Fe–4S]_P$ in AOXI (Fig. 2C and Fig. S2G, ESI†) showed a mixture of those in HRED and FOXI. To identify the crystallographically unassigned species, we performed *ab initio* electronic structure calculations to explore the molecular species, the most stable spin state and the configurations of O1 with the re-assignment of W2. We adopted six possible spin states[15] in each of the 12 structural models, where H_2O, OH^-, O^{2-}, O^-, SH^-, or S^{2-} were assigned to O1, and H_2O or OH^- were assigned to W2. For these 72 states, we performed geometry optimization, and identified the most stable structure as having O1 and W2 as OH^- and H_2O, respectively (Table S2 and Fig. S4, ESI†).

Structural changes around $[4Fe–4S]_P$ in S77HYB were perfectly reversible because HRED, AOXI, and FOXI had one cycle

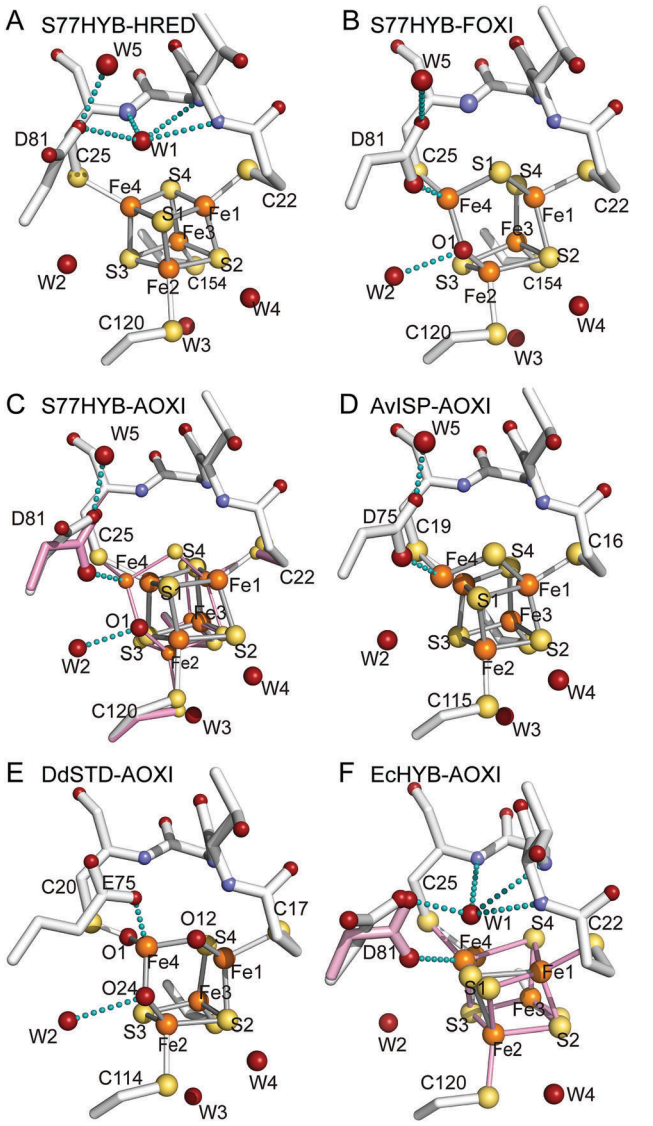

Fig. 2 Structures of $[4Fe–4S]_P$ of some [NiFe]-hydrogenases. (A, B, and C) S77HYB in the HRED, FOXI, and AOXI states, respectively. (D, E, and F) O_2-sensitive AvISP (PDB ID: 3MYR), DdSTD (PDB ID: 1E3D), and EcHYB (PDB ID: 6EHQ) in the AOXI states. Possible hydrogen-bonds are indicated by broken blue lines (atom colors are the same as Fig. 1). Five water molecules around $[4Fe–4S]_P$ are labeled as W1–W5. The atomic bonds in the conformer that appeared upon oxidation are depicted in pink in C and F.

of oxidation and reduction treatments (Table S1A, ESI†). This is attributed to the flexibility of Asp81 and movable W1. In contrast, the side chain of Glu75 of DvMSTD is too bulky to guarantee its reversible conformational changes (Fig. S1E, ESI†). $[4Fe–4S]_P$ of S77HYB is probably super-oxidized ($[4Fe–4S]_P^{3+}$) upon oxidation, although there is no direct experimental evidence, and supplies an additional electron to the active site to reduce O_2, as proposed for MBH-type enzymes. The structure in FOXI S77HYB suggests that the negative charges of Asp81 and OH^- possibly stabilize $[4Fe–4S]_P^{3+}$. The EPR Ni signals of AOXI S77HYB split apparently due to the spin–spin interaction between Ni^{3+} ($S = 1/2$) and $[4Fe–4S]_P^{3+}$ ($S = 1/2$) (Fig. S5A, ESI†). For FOXI S77HYB,

new EPR signals were observed at g = 1.93, 1.96, and 1.98, but the Ni signal splitting was not observed, which may be related with the X-ray structural data indicating conformational changes at $[4Fe–4S]_P$ (Fig. S5B, ESI†). For anaerobically purified DvMSTD, most enzymes were denatured by air-oxidation, whereas the EPR spectrum of FOXI DvMSTD did not exhibit prominent g = 1.93–1.98 signals (Fig. S5C and D, ESI†).

The structural elements found in S77HYB suggest that the concerted rearrangement of flexible $[4Fe–4S]_P$, Asp81, and water molecules may play an important role in protecting the active site from O_2 damage. However, another Hyb-type enzyme (Hyd-2) from *E. coli* (EcHYB), which has a 95% identical primary sequence to S77HYB (Fig. S6, ESI†), is O_2-sensitive.[16] $[4Fe–4S]_P$ in AOXI EcHYB showed the slightly deformed structure with a partially shifted Fe4 and the carboxy group of nearby Asp81 (Fig. 2F).[17] AvISP in Group 1e (47% identical to S77HYB) and STD-type enzyme from *D. desulfuricans* (DdSTD) (44% identical to S77HYB) are also O_2-sensitive, and $[4Fe–4S]_P$ in the AOXI state were deformed.[11,18] $[4Fe–4S]_P$ of AvISP and DdSTD in AOXI have a similar structure to those of AOXI and FOXI S77HYB, respectively (Fig. 2C–E). In AOXI S77HYB and AvISP, Fe4 of $[4Fe–4S]_P$ is shifted from the original position in a cubane $[4Fe–4S]_P$ and are within the coordination distance of the nearby carboxylate. It is still uncertain why $[4Fe–4S]_P$ of DdSTD had a deformed structure, even though it has a bulky Glu75, as in DvMSTD (Fig. S1E, ESI†). This question cannot be answered until the structure of HRED DdSTD is revealed. These structural features around $[4Fe–4S]_P$ found in various [NiFe]-hydrogenases indicate that an aspartate is preferable for reversible movement, but that it is not a prerequisite for assisting the reversible conformational change of $[4Fe–4S]_P$.

In addition to the flexibility of Asp81, S77HYB has a novel relocatable system for water molecules. To retrieve the activity of the inactive enzyme upon reduction, an oxygen ligand at the active site and an oxygen species (O1) of deformed $[4Fe–4S]_P$ must be expelled as H_2O. Thus, the enzyme requires a water escape pathway.[9,10,19] The water network including W1 (W1-net: W1–D81–W5–W6–water pool) is a potential route for water escape to restore the deformed $[4Fe–4S]_P$. In S77HYB, there is one loop (Gly18–Thr23) between W1-net and $[4Fe–4S]_P$ (Fig. 3A). Most O_2-sensitive enzymes have two bulky residues, a histidine at Gly18 (S77HYB) and a glutamate at Glu21 (S77HYB) (Fig. S6, ESI†), forming a "wall" between W1-net and $[4Fe–4S]_P$ and preventing the relocation of water molecules (Fig. 3B and Fig. S7A, B, ESI†). In contrast, because S77HYB has Gly18 instead of a histidine, O1 may escape easily. Our molecular dynamics (MD) simulations generated the distributions of the water molecules around $[4Fe–4S]_P$, suggesting that His13 in DvMSTD, but not Gly18 in S77HYB, disturbed water traffic between W1-net and $[4Fe–4S]_P$ (Fig. 3C and D). AvISP possesses Ser12 at Gly18 (S77HYB), but its Oγ immobilized W5 and W6 with hydrogen bonds (Fig. S6 and S7A, ESI†). The water traffic through this "wall" in O_2-tolerant enzymes may be disturbed by the bulky histidine residue (Fig. S7C, ESI†). However, these enzymes contain a novel $[4Fe–3S]_P$, and $[4Fe–3S]_P^{5+}$ can be mainly stabilized by a strong electron donor (N^-) rather than

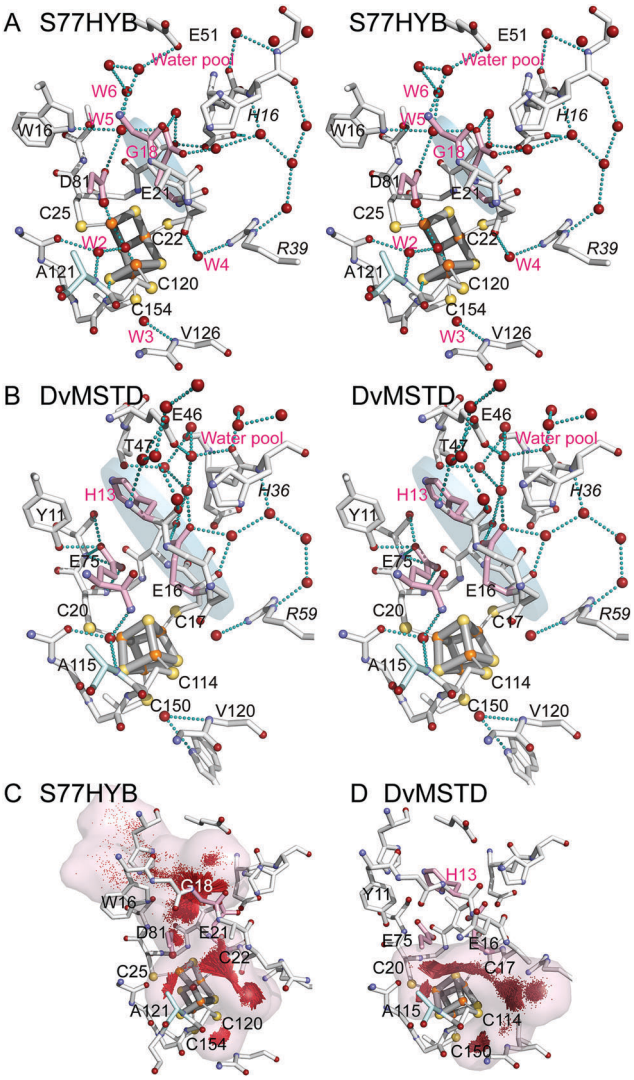

Fig. 3 (A and B) Stereo views of the water networks around $[4Fe–4S]_P$ of FOXI S77HYB and AOXI DvMSTD (PDB ID: 1WUI), respectively. Possible hydrogen-bonds are indicated by broken blue lines. The "wall" (a gray disc) formed by the loop (Gly18–Thr23) would control the water molecule traffic between W1-net (W1–D81–W5–W6–water pool) and $[4Fe–4S]_P$. The residue in the large subunit are labeled in italics, and the water molecules are labeled in red. (C and D) Water distribution (shown by red points) in the cavity (shown in light pink) obtained by MD simulations of S77HYB and DvMSTD, respectively. The atomic bonds of G18, E21, and D81 (S77HYB) and H13, E16, and E75 (DvMSTD) are shown in pink, whereas those of A121 (S77HYB) and A115 (DvMSTD) are shown in cyan (atom colors are the same as Fig. 1).

carboxylate or OH^-. An additional oxygen species (OH^-) attached to Fe1 (facing in another direction) of $[4Fe–3S]_P$ in ReMBH may use another water escape route (Fig. S7C, ESI†).[19,20] Although EcHYB has a small "wall" as in S77HYB, it is not O_2-stable. $[4Fe–4S]_P$ in AOXI was a mixture of the original cubane form and the deformed structure. Fe4 in the deformed cluster was coordinated by Asp81, but OH^-, which was found in AOXI and FOXI S77HYB, was not incorporated between Fe2 and Fe4, indicating that the deformed structure of $[4Fe–4S]_P$ of EcHYB was different from that of S77HYB. In EcHYB,

Ala121 near W2 in S77HYB is replaced by Ser121. Since Ser121 is located in the other side of the water escape route from $[4Fe–4S]_P$, this replacement would not directly influence the water distribution. W2 in S77HYB is hydrogen-bonded to the nearby carbonyl O (Ile154) and amide N (Ala121), whereas that in EcHYB is additionally supported by Oγ of Ser121 (Fig. S7A and D, ESI†). In addition, the Oγ atom occupies the space next to W2. As a result, the A121S replacement would disturb the flexibility of $[4Fe–4S]_P$. [NiFeSe]-hydrogenase from *D. vulgaris* Hildenborough (Group 1a), which was reported to be O_2-tolerant, showed similar structural features at around $[4Fe–4S]_P$ in the AOXI state, suggesting that there is a universal O_2-tolerance mechanism, although a different system has been proposed based on the novel Se ligand at the active site.[21] In addition, it has recently been reported that Ni in the active site of NAD^+-reducing [NiFe]-hydrogenase (Group 3d) in the AOXI state is coordinated by the nearby glutamate that would protect O_2 access.[22]

We propose a novel molecular mechanism for protecting the active site from O_2 damage in S77HYB (Fig. S8, ESI†). The fundamental principle (additional electron donation from the proximal Fe–S cluster to the Ni–Fe active site) is probably the same as in MBH-type enzymes, but the molecular mechanism is slightly different. In S77HYB, we propose that $[4Fe–4S]_P$ is super-oxidized to the $[4Fe–4S]_P^{3+}$. We also propose that this oxidation results in the shift of Fe4, concomitant with coordination by nearby Asp81 and OH^- between Fe2 and Fe4. Upon reduction, deformed $[4Fe–4S]_P^{3+}$ is immediately restored to its original cubane configuration with the concomitant relocation of water molecules. O_2-sensitive enzymes do not have an electron supply system or water relocation system for water escape to restore the deformed cluster. Because the redox potential of $[4Fe–4S]_P$ might be not sufficiently high compared with those of $[4Fe–3S]_P$ in MBH-type enzymes, the medial cluster, $[3Fe–4S]_M$, which has a high potential, may play a crucial role in the back donation series of the electrons to the Ni–Fe active site.[23] The molecular system for protecting the active site from O_2 damage found in S77HYB is an intermediate mechanism that links those of O_2-sensitive (STD-type) and O_2-tolerant (MBH-type) [NiFe]-hydrogenases.

This work was supported by Japan Science and Technology Agency CREST grant JPMJCR12M4 (Y. H. and S. H.), Japan Society for Promotion of Science Category B, No. 25291038 (Y. H.) and 25287099 (M. T.), Challenging Exploratory Research, No. 24657077 (Y. H.), Scientific Research on Innovative Areas, No. JP15H00945 (S. H.), Young Scientists B No. JP16K17936 (H. T.); and Specially Promoted Research No. 26000008 (S. O.), and by research grants from The Mitsubishi Foundation (Y. H.) and the ENEOS Hydrogen Trust Fund (Y. H.). We thank Drs K. Kano, Y. Kitazumi, N. Shibata, and T. Hiromoto for their helpful discussions, and Ms K. Hataguchi and Ms K. Matsumoto for their bacterial cultures.

Conflicts of interest

There are no conflicts of interest to declare.

Notes and references

‖ Atomic coordinates and structure factors for the reported structures have been deposited in the Protein Data Bank with the accession codes 5XVB (HRED), 5XVC (FOXI) and 5XVD (AOXI) for the *Citrobacter* sp. S-77 enzyme and 5Y34 (FOXI) for the *Hydrogenovibrio marinus* enzyme.

1 P. M. Vignais and B. Billoud, *Chem. Rev.*, 2007, **107**, 4206–4272.
2 C. Greening, A. Biswas, C. R. Carere, C. J. Jackson, M. C. Taylor, M. B. Stott, G. M. Cook and S. E. Morales, *ISME J.*, 2016, **10**, 761–777.
3 H. Ogata, S. Hirota, A. Nakahara, H. Komori, N. Shibata, T. Kato, K. Kano and Y. Higuchi, *Structure*, 2005, **13**, 1635–1642.
4 W. Lubitz, E. Reijerse and M. van Gastel, *Chem. Rev.*, 2007, **107**, 4331–4365.
5 Y. Higuchi, T. Yagi and N. Yasuoka, *Structure*, 1997, **5**, 1671–1680.
6 V. M. Fernandez, E. C. Hatchikian, D. S. Patil and R. Cammack, *Biochim. Biophys. Acta*, 1986, **883**, 145–154.
7 J. A. Cracknell, A. F. Wait, O. Lenz, B. Friedrich and F. A. Armstrong, *Proc. Natl. Acad. Sci. U. S. A.*, 2009, **106**, 20681–20686.
8 Y. Shomura, K.-S. Yoon, H. Nishihara and Y. Higuchi, *Nature*, 2011, **479**, 253–257.
9 J. Fritsch, P. Scheerer, S. Frielingsdorf, S. Kroschinsky, B. Friedrich, O. Lenz and C. M. T. Spahn, *Nature*, 2011, **479**, 249–252.
10 A. Volbeda, P. Amara, C. Darnault, J.-M. Mouesca, A. Parkin, M. M. Roessler, F. A. Armstrong and J. C. Fontecilla-Camps, *Proc. Natl. Acad. Sci. U. S. A.*, 2012, **109**, 5305–5310.
11 H. Ogata, P. Kellers and W. Lubitz, *J. Mol. Biol.*, 2010, **402**, 428–444.
12 S. Eguchi, K.-S. Yoon and S. Ogo, *J. Biosci. Bioeng.*, 2012, **114**, 479–484.
13 N. D. Muhd Noor, K. Nishikawa, H. Nishihara, K.-S. Yoon, S. Ogo and Y. Higuchi, *Acta Crystallogr., Sect. F: Struct. Biol. Commun.*, 2016, **72**, 53–58.
14 H. Ogata, K. Nishikawa and W. Lubitz, *Nature*, 2015, **520**, 571–574.
15 J. Kim, J. Kang, H. Nishigami, H. Kino and M. Tateno, *J. Phys. Soc. Jpn.*, 2018, **87**, 034804.
16 M. J. Lukey, A. Parkin, M. M. Roessler, B. J. Murphy, J. Harmer, T. Palmer, F. Sargent and F. A. Armstrong, *J. Biol. Chem.*, 2010, **285**, 3928–3938.
17 S. E. Beaton, R. M. Evans, A. J. Finney, C. M. Lamont, F. A. Armstrong, F. Sargent and S. B. Carr, *Biochem. J.*, 2018, **475**, 1353–1370.
18 P. M. Matias, C. M. Soares, L. M. Saraiva, R. Coelho, J. Morais, J. L. Gall and M. A. Carrondo, *J. Biol. Inorg. Chem.*, 2001, **6**, 63–81.
19 I. Dance, *Chem. Sci.*, 2015, **6**, 1433–1443.
20 S. Frielingsdorf, J. Fritsch, A. Schmidt, M. Hammer, J. Löwenstein, E. Siebert, V. Pelmenschikov, T. Jaenicke, J. Kalms, Y. Rippers, F. Lendzian, I. Zebger, C. Teutloff, M. Kaupp, R. Bittl, P. Hildebrandt, B. Friedrich, O. Lenz and P. Scheerer, *Nat. Chem. Biol.*, 2014, **10**, 378–385.
21 M. C. Marques, C. Tapia, O. Gutiérrez-Sanz, A. R. Ramos, K. L. Keller, J. D. Wall, A. L. De Lacey, P. M. Matias and I. A. C. Pereira, *Nat. Chem. Biol.*, 2017, **13**, 544–550.
22 Y. Shomura, M. Taketa, H. Nakashima, H. Tai, H. Nakagawa, Y. Ikeda, M. Ishii, Y. Igarashi, H. Nishihara, K.-S. Yoon, S. Ogo, S. Hirota and Y. Higuchi, *Science*, 2017, **357**, 928–932.
23 R. M. Evans, A. Parkin, M. M. Roessler, B. J. Murphy, H. Adamson, M. J. Lukey, F. Sargent, A. Volbeda, J. C. Fontecilla-Camps and F. A. Armstrong, *J. Am. Chem. Soc.*, 2013, **135**, 2694–2707.

